European Polymer Journal 199 (2023) 112434

Contents lists available at ScienceDirect

European Polymer Journal

journal homepage: www.elsevier.com/locate/europolj

Microscale dynamics in thermoreversible hydrogels: Impact of probe size and concentration

Hengwei Zhu [a], Suan P. Quah-Ivarson [a], Yugang Zhang [b], Andrei Fluerasu [b], Xiaoxi Yu [a], Bingqian Zheng [a], Xuechen Yin [a], Weiping Liu [a], Surita R. Bhatia [a,*]

[a] Department of Chemistry, Stony Brook University, Stony Brook, NY 11794-3400, United States
[b] National Synchrotron Light Source II, Brookhaven National Laboratory, Upton, NY 11973, United States

ARTICLE INFO

Keywords:
Nanoparticles
Biomaterials
Gels
Scattering
Rheology

ABSTRACT

Passive microrheology techniques using dynamic light scattering (DLS) and X-ray photon correlation spectroscopy (XPCS) have emerged as important techniques for characterizing the dynamics and viscoelastic properties of soft polymeric biomaterials. However, the impact of probe particle type, size, and concentration are important considerations in interpretation of results and comparison to properties obtained from bulk rheology measurements. In this work, we investigate a model thermoreversible polymeric hydrogel and compare results from DLS-microrheology with different size and concentrations of polystyrene probe particles and XPCS-microrheology with inorganic nanoparticles. We obtained trends that aligned most closely with the macroscopic rheology with probe particles that are slightly larger than the characteristic length scale of the gel structure, but within the same order of magnitude. By contrast, larger probe particles yielded microrheology data that are more dominated by elastic behavior than what we might expect from bulk rheology experiments, while use of small inorganic nanoparticles in XPCS-microrheology resulted in a more a more viscous response than would be expected based on the bulk rheology. This study demonstrates the utility of passive DLS- and XPCS-based microrheology in characterizing the rheological properties of complex polymeric biomaterials, while also highlighting important considerations in experimental design and choice of type, size, and concentration of probe particles used.

1. Introduction

The viscosity, elasticity, and dynamics of soft materials and complex fluids are crucial to their applications in foods [1–3], pharmaceutical processing and drug delivery [4–6], protein-based therapeutics [7,8], and bioprocessing [9,10]. Rheometry is often used to quantify these physical properties. However, conventional oscillatory rheometry requires a large sample volume, and the upper frequency range is limited [11]. Additionally, external perturbations during measurements may destroy the microstructure of materials. Microrheology is a newer approach that can probe the viscoelasticity of materials on small length scales by measuring the motion of probe particles. Many different microrheology techniques have been developed during the past two decades [12–18], and they can be classified into passive or active microrheology based on the driving force of particle motion. Dynamic light scattering (DLS)-microrheology is a type of passive microrheology which follows the motions of probe particles that arise from thermal fluctuations [19]. The thermal motion can be presented as the mean square displacement (MSD) over time, and the complex modulus can then be calculated from MSD via Generalized Stokes-Einstein Relation (GSER) [17,18]. DLS-microrheology offers many advantages, including only requiring small sample volumes (μL level) and enabling measurements at frequencies up to 10^6 Hz within short acquisition times.

A similar approach to passive microrheology can be used with X-ray photon correlation spectroscopy (XPCS), a powerful tool for microstructural dynamic studies. Similar to DLS with visible light, XPCS traces the fluctuations in coherent intensity of scattered X-rays to provide information about material dynamics. The much shorter wavelength of X-rays allows XPCS to probe motions over significantly shorter distances, giving it access to smaller length scales and longer time scales that are outside the capabilities of DLS. XPCS can be used to access structural dynamics over length scales from nanometers to hundreds of nanometers, and time scales from milliseconds to hundreds of seconds. XPCS can also be applied to cloudy and opaque materials, which are challenging or

* Corresponding author.
E-mail address: surita.bhatia@stonybrook.edu (S.R. Bhatia).

https://doi.org/10.1016/j.eurpolymj.2023.112434
Received 3 July 2023; Received in revised form 15 September 2023; Accepted 16 September 2023
Available online 21 September 2023

impossible to characterize by DLS.

In addition to probing different time scales, different sizes and types of probe particles are typically used in DLS- and XPCS-based microrheology studies of polymers and biomaterials. For DLS-microrheology, a probe particle that is different in size than the characteristic structural length scale of the system is often used, in order to selectively analyze channels that correspond to the motion of the probe particles. This is convenient for data analysis but precludes use of the technique to explore microrheological properties on some length scales. Polymeric latexes are often used as probe particles, as these scatter light well, with polystyrene microspheres being a common choice. Polystyrene microspheres can be modified to obtain positive, negative or neutrally charged surfaces [20] to aid in homogeneous dispersion in solutions and gels, which helps ensure single scattering [21]. By comparison, for XPCS-based microrheology, inorganic nanoparticles offer the advantages that they scatter X-rays strongly and have a size scale that corresponds well with the length scale probed by XPCS. Because inorganic nanoparticles scatter X-rays much more strongly than polymers and biomolecules, the signal will be dominated by scattering from the probe particles, and it is possible to use probe particles that are similar in size to the characteristic structural length scale of the gel.

In both cases, the size of the probe particles is an important factor in interpreting the viscoelastic parameters that are measured and how they correspond to the bulk rheological properties measured in a conventional oscillatory rheology experiment. The size of probe particles influences the thermal motion, and small probe particles decorrelates more quickly [21]. Additionally, the size of the probe particle in relation to the structural length scales of the material can determine whether the probe particle motion is representative of the bulk viscoelasticity or local viscoelastic properties. For relatively simple fluids such as polymer solutions, there is often a good agreement between properties measured via microrheology and bulk properties measured using oscillatory rheology [17]. However, the situation is more complex for gels with heterogenous or multiscale structure; for instance, if the probe particle is smaller than length scales such as the mesh size of a polymeric gel, the properties can be quite different on the microscale as compared to the macroscale. Our previous XPCS-microrholeogy studies of alginate-block copolymer composite gels with inorganic nanoparticles showed that microrheology analysis yielded similar trends with temperature as the bulk properties, but storage and loss moduli values that were orders of magnitude lower than traditional bulk rheology measurements, strongly suggesting a difference in rheological behavior on the micro vs macro scale [22].

In this study, we present results from DLS-microrheology with different size of polystyrene probe particles and XPCS-microrheology with inorganic nanoparticles, applied to a model thermoresponsive gel that has been well-studied by bulk rheology, aqueous gels of poly (ethylene oxide)-*b*-poly(propylene oxide)-*b*-poly(ethylene oxide) (PEO-PPO-PEO), a nonionic amphiphilic triblock copolymer [23]. Pluronic® F127 (F127) is one of a family of commercially-available PEO-PPO-PEO copolymers with the approximate formula PEO_{100}-PPO_{65}-PEO_{100}. The difference in hydrophilicity between poly(ethylene oxide) (PEO) and poly(propylene oxide) (PPO) enables F127 form micelles in aqueous environments [24–26], with a micellar diameter of about 11 nm. Hydrophobic PPO forms a compact micelle core while the hydrophilic PEO chains are the corona or shell. This self-assembly behavior can be driven by temperature. When aqueous F127 solutions reach the lower gelation temperature, micelles start to be ordered and pack into a cubic structure, eventually forming a strong gel. As temperature continues to increases to the upper gelation temperature, the solubility of PEO in water decreases, increasing the size of the insoluble micelle core and modifying the structure of the gel phase [24,27].

For the microrheology results presented later, it is helpful to consider characteristic length scales in this system. In addition to the 11 nm diameter of the micelles themselves, as described above, in the gel state F127 micelles form a cubic structure. In the gel state, the micelles adopt an FCC packing. This results in a interstitial spacing of approximately 4.5–8 nm in the gel. It is also possible to estimate an effective "mesh size" of the gel state using the plateau modulus; this analysis results in an estimated mesh size of 6 nm. However, it is not clear if it is appropriate to apply this to F127 gels, since these are physical gels for which a mesh size is not well-defined. In either case, however, the characteristic length scales for structure within the gel are in the range of 4.5–11 nm.

F127 has been widely studied for drug delivery, as the PPO core is desirable for incorporating drugs, and the thermoresponsive properties of the gel can help control the delivery process [28–30]. Our results show that size and concentration of probe particles has a significant influence on MSD and thus influence viscoelasticity results. In addition, size of probe particles affects quality of the data collected at some concentration or temperature of F127 solution. These have implications for interpretation of XPCS- and DLS-microrheology results on polymeric gels and biomaterials and design of future experiments for studying dynamics of these systems.

2. Materials and methods

2.1. Materials

Various sizes of carboxyl-modified polystyrene (PS) probe particles in aqueous suspensions were obtained from Invitrogen and cell culture grade Pluronic® F127 was purchased from Sigma-Aldrich and were utilized for the DLS experiments. For the XPCS experiments, 12 nm silica nanoparticles (Ludox) were obtained from Grace.

2.2. Pluronic® F127 solution preparation

Pluronic® F127 solutions of 15, 20, 25, and 30 wt% were prepared with nano pure water (purified by a Thermo Scientific Barnstead NanoPure Infinity filtration system). The respective amounts of Pluronic® F127 were dissolved in nano pure water and stirred for 4 h. Polystyrene probe particles with diameters of 40 nm, 100 nm, 500 nm, and 2 μm were added to the Pluronic® F127 solution for DLS measurement, respectively. Two drops of a stock probe particle solution were added to 4 g of the Pluronic® F127 solution to obtain final probe particle concentrations of 0.06–0.07 wt%. For the series of experiments exploring the effect of probe particle concentration, the probe particle stock solution was diluted 20 or 100 times, leading to probe particle concentrations of 0.003 wt% and 0.0007 wt%, respectively. For XPCS measurements, 12 nm diameter SiO_2 particles were added to 30 wt% Pluronic® F127 solution. To estimate the viscoelastic moduli via the GSE equation, F127 samples are treated as a continuum around PS probe particles.

2.3. Dynamic light scattering (DLS) and bulk rheology

Dynamic light scattering (DLS) experiments were performed using a Brookhaven Instruments Nanobrook Omni light scattering instrument with a red diode laser with a 617 nm wavelength, capable of measuring a minimum displacement of 1.0 nm. Measurements were performed at an incident angle of 90°. Samples were measured between 15 and 40 °C in increments of 2.5 °C and each face of the cuvettes were measured 3 times, for a total of 12 measurements that were averaged. The full ensemble average of autocorrelation function over spatial position can eliminate the influence of scattering intensity caused by non-ergodic materials. After reaching each temperature, samples were allowed to equilibrate for 5 min before the measurements were started. For comparison with DLS microrheology results, conventional oscillatory rheology experiments, or bulk rheology measurements, were performed on an TA Instruments DHR-III rheometer using a 40 mm parallel plate geometry.

2.4. X-ray photon correlation spectroscopy (XPCS)

Dynamic studies were performed at the coherent hard X-ray (CHX, 11-1D) beamline at the National Synchrotron Light Source II (NSLS-II) located at Brookhaven National Laboratory, Brookhaven, NY. The X-ray energy was set to 9.65 keV (1.29 Å wavelength) delivered by a 3-meter long in-vacuum undulator with 20 mm magnetic period and a double-crystal monochromator. A partially coherent X-ray beam with a flux at the sample of ~ 1011 photon/sec and a focused beam size of 10 × 10 μm^2 was achieved by focused with a set of Be Compound Refractive Lenses and a set of Si kinoform lenses in front of the sample. The detector-sample distance was set to 4.91 m with 0.036 transmission of the full beam and an exposure time of 37.2 ms. The X-ray radiation dose on the sample was controlled by a millisecond shutter and filters of different thickness of silicon wafers. The data acquisition strategy was optimized to ensure that the measured dynamics and structure are dose independent. Measurements were taken in a temperature-controlled environment in the 10–80 °C temperature range. To increase the signal to noise, the one-time correlation functions reported in this study are an average of 10 measurements at each temperature.

2.5. Microrheology

The Brownian motion of the micelles were monitored using DLS and XPCS. The mean-squared displacement (MSD), $\langle \Delta r^2(t) \rangle$, was extracted from the auto-correlation function, $g_2(q,t)$, as follows

$$g_2(q,t) = 1 + b\exp\left[-q^2\langle \Delta r^2(t)\rangle/3\right] \quad (1)$$

where q is scattering vector and $b = (g_2(0) - 1)$ such that $g_2(0)$ is the auto-correlation function at small delay times τ. The MSD can be related to the frequency-dependent complex shear modulus (G^*) of the surrounding fluid through the generalized Stokes-Einstein relation [31,32],

$$G^*(\omega) = \frac{k_B T}{\pi a \langle \Delta r^2(t)\rangle \Gamma(1+\alpha(\omega))} \quad (2)$$

where k_B is Boltzmann constant and a is the radius of probe particle. To evaluate this, we used the power-law approximation described by Furst and Squires [33] where the MSD at each sampled time t_0 is a power-law function,

$$\langle \Delta r^2(t)\rangle \approx \langle \Delta r^2(t_0)\rangle (t/t_0)^{\alpha(t_0)} \quad (3)$$

where α is the logarithmic slope of the mean-squared displacement evaluated at t_0,

$$\alpha(t_0) = \left.\frac{d(ln\langle \Delta r^2(t)\rangle)}{d(\ln(t))}\right|_{t=t_0} \quad (4)$$

The Fourier Transformation of the power-law yields the modulus amplitude,

$$|G^*(\omega_0)| = \left.\frac{Dk_B T}{3\pi R\langle \Delta r^2(t_0)\rangle \Gamma[\alpha(t_0)+1]}\right|_{t=1/\omega_0} \quad (5)$$

where D represents the number of dimensions tracked for the MSD. Using G^*, the viscous loss modulus (G'') and the elastic storage modulus (G') can be obtained by [31,32]

$$G'' = G^*(\omega)^*\sin\left(\frac{\alpha(\omega)\pi}{2}\right) \quad (6)$$

$$G' = G^*(\omega)^*\cos\left(\frac{\alpha(\omega)\pi}{2}\right) \quad (7)$$

3. Results and discussion

3.1. DLS-microrheology probe size dependence

In exploring the complex viscosity results using different size probe particles, we observed that size of probe particles influences the measurement results, as shown in Fig. 1. When the size of the probe particle is 40 nm (Fig. 1a), the complex viscosity of 15 wt% F127 showed minimal frequency dependence at lower temperatures (15–20 °C) over the measurable frequency range, indicative of liquid-like behavior, with a more significant frequency dependence at higher temperatures (25–40 °C) in the high frequency range, indicating viscoelastic behavior. By comparison, when the size of probe particle is 100 nm (Fig. 1b), the complex viscosity of 15 wt% F127 showed low frequency dependence within whole frequency range over all temperatures, indicative of a liquid-like behavior overall. For larger probe particles (500 and 2000 nm), as shown in Fig. 1c and 1d, they also show some frequency dependence at low frequency range (below 1000 rad/s), indicating viscoelastic behavior, while at higher frequency range the data become noisy, especially for 2000 nm results. This may be an artifact due to the concentration of probe particles; we discuss this further below and in Section 3.2. The trends observed in DLS-microrheology with the 40 nm probe particle (Fig. 1a) are most similar to what is seen in bulk rheology experiments on samples at this polymer concentration and temperature range (Fig. S1); samples of 15 wt% F127 in water typically begin to show formation of a weak gel close to 40 °C. The measurable frequency ranges for DLS microrheology, bulk rheology, and XPCS microrheology vary, making direct comparisons over a wide frequency range difficult. However, within the range of frequencies that overlap for bulk rheology and DLS microrheology, the complex viscosity demonstrates similar trends only for samples that are strong gels, well past the gel point (Fig. S8c), while no similar trend is observed for weaker gels that are close to the gel point (Fig. S8a and S8b). It is noticeable that the moduli results from microrheology are 4–5 orders of magnitude lower than results from bulk rheology. This difference makes the effects of different size probe particles less obvious when comparing the results of microrheology and bulk rheology.

When the temperature increased to 40 °C, the scaled MSD of the experiments performed with 40 and 100 nm diverge at low lag times, and the exponent of 40 nm probe at low lag time decreases (Fig. 2c), corresponding to the overlap of G' and G'' at high frequency in Fig. 3c. This may be due to the gel transition of 15 wt% F127 at this temperature. Therefore, the gelation behavior is only detected on the smallest length scale, while the material is still dominated by viscous loss on larger length scales. It is notable that the diffusive exponent value of the 2000 nm probe particle is between 0 and 0.5 for all temperatures, which means that motion of the 2000 nm particles is hindered at all temperatures explored here. This behavior typically arises from elastic effects in the polymer gel; however, the G' and G'' in Fig. 3 indicates that the rheological response is dominated by viscous effects. The origin of the hindered motion of the 2000 nm particles is unclear; it may arise from particle-particle interactions or interactions between particles and individual micelles. If this is the case, decreasing the concentration of probe particles may yield more reliable microrheology results. In Section 3.2 we explore this further by utilizing 2000 nm probe particles at lower particle concentrations.

F127 systems at higher polymer concentrations also show different microrheology results when using probe particles of different sizes, as shown by the results on 20 wt% F127 in water. As shown in Figs. 4a and 5a, for 40 and 100 nm probe particles, the scaled MSD overlaped well at 15 °C, and the material is dominated by a viscous response. The plateau in the scaled MSD between 10^2 and 10^4 μs for 2000 nm probe particles in Fig. 4a corresponds to the overlap of G' and G'' in Fig. 5a, indicating gel formation at 15 °C, which is also observed in the bulk rheology for this concentraiton of F127 (Fig. S5). When the temperature is increased to 22.5 °C, gel behavior is observed for all size probes except the 100 nm

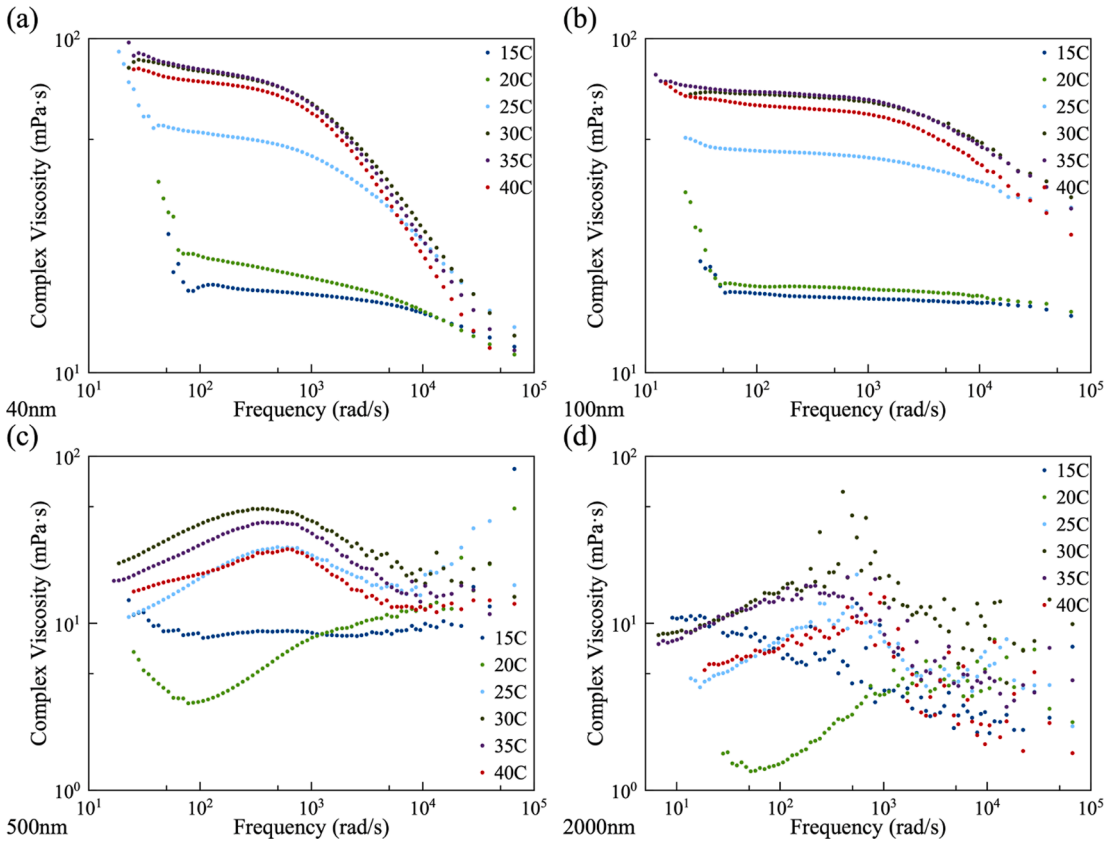

Fig. 1. Complex viscosity from of DLS-microheology on 15 wt% F127 with probe particles of diameter a) 40 nm, b) 100 nm, c) 500 nm, and d) 2000 nm, from 15 to 40 °C.

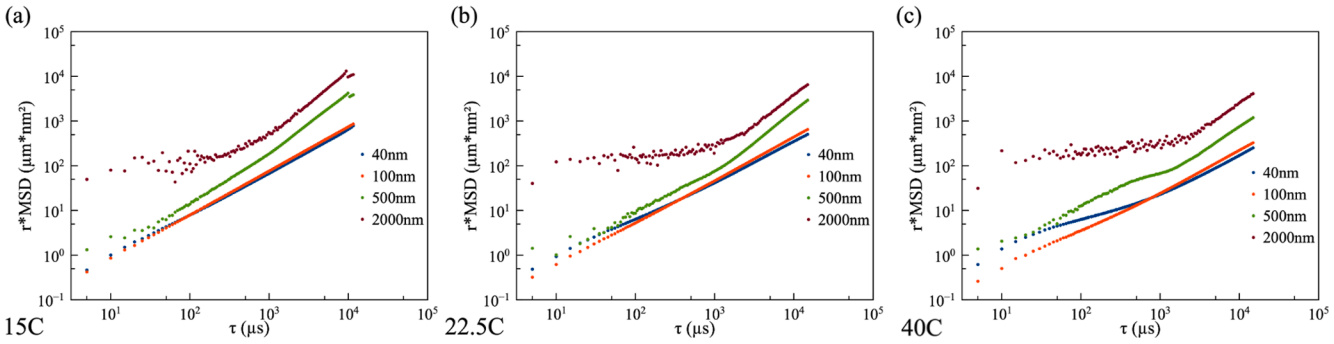

Fig. 2. Scaled MSD for various probe particle sizes in 15 wt% F127 at temperatures of a) 15 °C, b) 22.5 °C, and c) 40 °C.

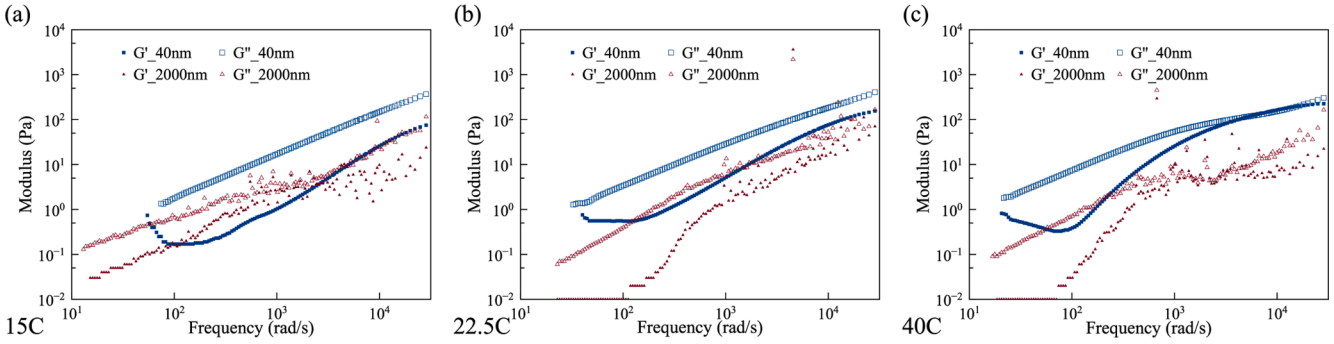

Fig. 3. Storage and loss modulus for 40 nm and 2000 nm probe particles in 15 wt% F127 at temperatures of a) 15 °C, b) 22.5 °C, and c) 40 °C.

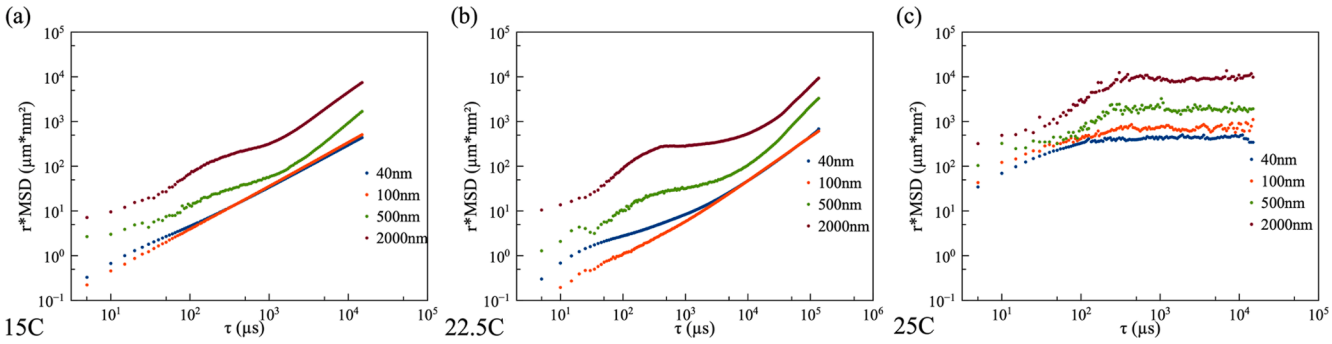

Fig. 4. Scaled MSD for various probe particle sizes in 20 wt% F127 at temperatures of a) 15 °C, b) 22.5 °C, and c) 25 °C.

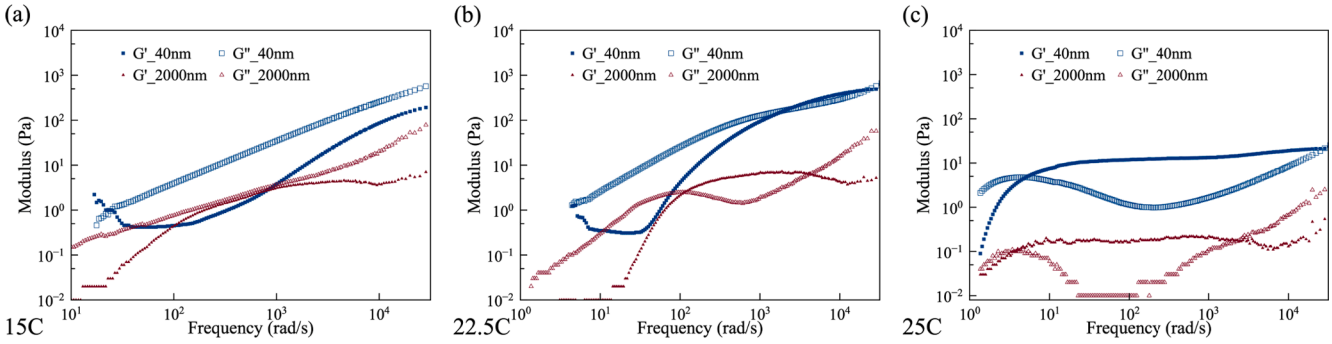

Fig. 5. Storage and loss modulus for 40 nm and 2000 nm probe particles in 20 wt% F127 at temperatures of a) 15 °C, b) 22.5 °C, and c) 25 °C.

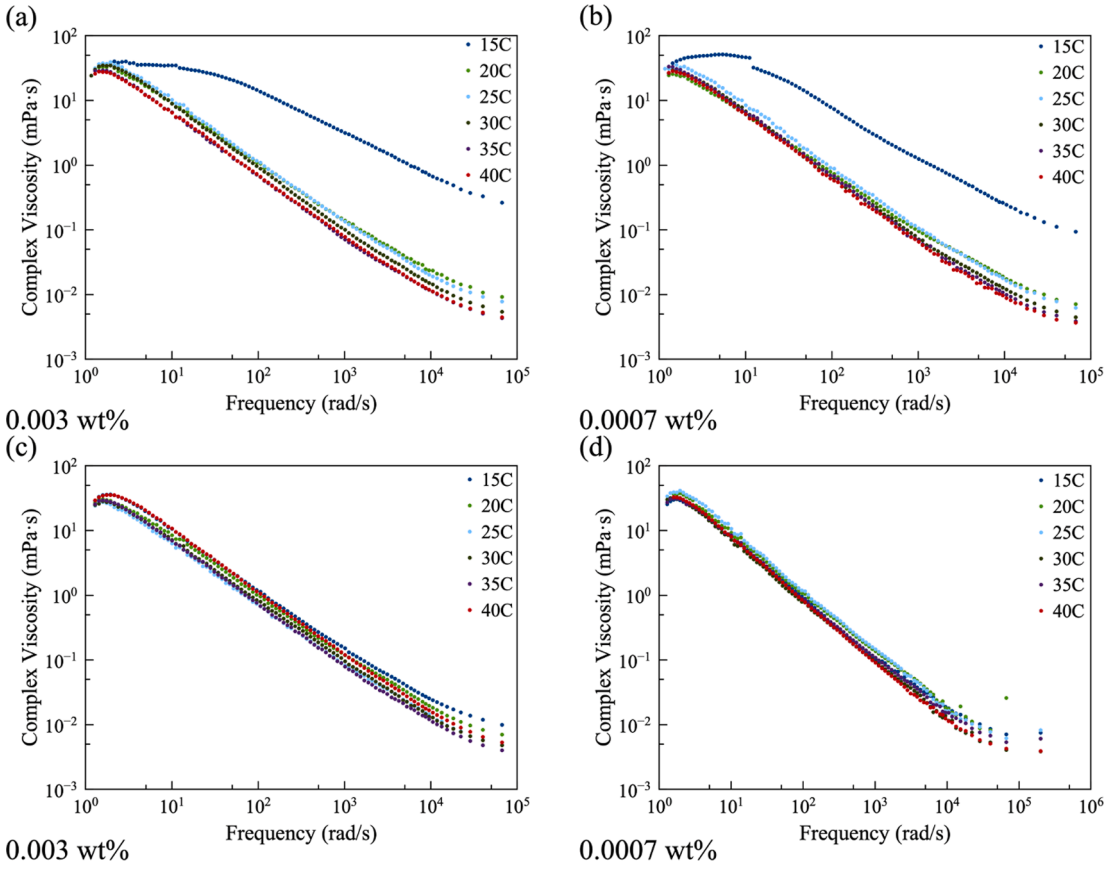

Fig. 6. Complex viscosity from DLS-microrheology at temperatures of 15–40 °C with probe particles of diameter of 2000 nm for a) 25 wt% F127 with 0.003 wt% probe particles, prepared from a probe particle stock solution diluted 20 times, b) 25 wt% F127 with and 0.0007 wt% probe particles, prepared from a probe particle solution diluted 100 times, c) 30 wt% F127 with 0.003 wt% probe particles, and d) 30 wt% F127 with 0.0007 wt% probe particles.

probe. As temperature is further increased to 25 °C, the material is elastically dominated except the low frequency range. It may be that trapped probe particles can 'escape' from their gel cage at long lag times, as F127 hydrogels are physical gels and dynamic in nature, as opposed to chemically crosslinked networks in which probe particles remain trapped by the elastic network [34]. In addition, even though microrheology can be used to detect the transitions between liquid and gel states, there are differences between the bulk rheology and microrheology (Figs. S4 and S5). We attribute these to the different length scales probed by the two techniques. For weak gels very near the gel point, samples exhibit gel-like behavior in the bulk macroscale rheology experiments, while displaying liquid-like behavior in microrheology. When samples become strong gel, G' and G'' behaviors are consistent between bulk rheology and microrheology (Figs. S6 and S7), as in strong gel state, samples perform gel-like behavior on both microscale and macroscale.

3.2. DLS-microrheology probe concentration dependence

Initial data collected on 15 wt% F127 samples with 2000 nm probe particles at particle concentrations of 0.07 wt% led to noisy data (Fig. 1d); similarly noisy results were obtained for samples at 25 wt% and 30 wt% F127. We attempted to overcome this issue by diluting the stock solution of 2000 nm probe particles 20 and 100 times to see if this would improve our measurements. As shown in Fig. 6, complex viscosity data collected using 2000 nm particles at these lower particle concentrations were much cleaner. Additionally, solutions prepared with particle concentrations of 0.003 wt% and 0.0007 wt% did not show significant differences between each other in the results for DLS-microrheology on 25 wt% F127 samples.

However, when the concentration was changed to 20 wt%, different probe particle concentrations yielded various MSD results, especially in the low temperature range before the sample undergoes gelation. This indicates that the concentration of probe particles can impact the microrheology results when F127 systems are in the sol state. As the temperature increased, the F127 became a gel and the concentration of the probe particles no longer affected the measurement. As described above, there may be some interactions between probe particles and individual micelles that impacts particle motion when the F127 systems are in the sol state; once in the gel state, the dynamics of probe particles are dominated by the hindered motion in the gel (see Fig. 7).

3.3. XPCS microrheology

We also employed X-ray photon correlation spectroscopy (XPCS) microrheology techniques to investigate the behavior of F127 at smaller lengths scales and longer time scales. In these studies, smaller SiO_2 particles (12 nm diameter) were used to probe the dynamics of systems containing 30 wt% F127. For these measurements, the size of the probe particles is very similar in size to the F127 micelles themselves, approximately 11 nm in diameter (Fig. S10). As discussed above, there are additional relevant length scales for the gels, although they are on the same order as the micelle size; we expect the interstitial spaces in the cubic gels to be 4.5–8 nm, and an effective mesh size for 30 wt% F127 can be estimated as 6 nm, using the relationship $G_0 = K_B T/\xi^3$, where ξ is the mesh size and G_0 is the elastic plateau modulus from Fig. S9. It should be noted that an effective mesh size calculated this way will vary with temperature for these thermoresponsive gels, and it is not clear if it is appropriate to use the concept of a mesh size for physical gels such as these.

The complex viscosity of 30 wt% F127 at temperatures between 10 °C and 80 °C are reported in Fig. 8a. We observed viscoelastic behavior with 30 wt% F127 at temperatures between 10 °C and 80 °C as indicated by the frequency-dependent complex viscosity. The results show a distinct difference in viscous behavior between 10 and 30 °C and 40–80 °C. At lower temperatures of 10–30 °C, we observe lower complex viscosity values while at higher temperatures of 40–80 °C, we observe higher complex viscosity values with a slightly steeper frequency-dependent slope. The difference in viscosity behavior here indicates that, at the microscale, the system shows a transition from a viscoelastic liquid to a viscoelastic solid between 30 °C and 40 °C. However, studies in the past that have used bulk rheology such as the study done by Liu *et al.* have found that the critical gelation temperature (CGT) of 30 wt% F127 falls around 15–18 °C; [24] thus, based on bulk rheology we would expect the transition in the range of 15–18 °C rather than 30–40 °C. This significant difference in gelation temperature between bulk rheology and microrheology is further evidence that polymeric gels can exhibit different rheological properties in their micro and macro environments, and that understanding both of these behaviors are essential in characterizing these materials.

We also observed several interesting behaviors at the transition temperatures of 30 wt% F127 using the 12 nm SiO_2 probe particles. In Fig. 8b, the MSD of 30 wt% F127 over time displayed a distinguishable difference between the movement of the probe particles at lower temperatures versus higher temperatures. At lower temperatures, the probe particles are diffusing more freely as indicated by the increasing MSD over time and becomes restricted in motion as the MSD starts to a plateau around 8.3×10^6 μs at about 1300 nm^2. This behavior is expected here because F127 micelles are able to move freely at lower temperatures, which allow the probe particles to also diffuse freely within the medium. At higher temperatures, the MSD increases much more slowly and starts to plateau much sooner around 1.2×10^6 μs at a lower MSD of about 300 nm^2, indicating greater restriction in movement from ordered micellar structures. However, the MSD deviates from these two general trends at 10 °C and 40 °C. At 10 °C, where we expected the probe particles to be most freely diffusing, we see that the probe particles are diffusing quite slowly through the polymer network. We believe that this occurrence is due to the temperature being close to the critical micellization temperature (CMT) of 30 wt% F127, which has been reported to be around 9 °C [24,35]. At 10 °C, the polymer solution is likely to be made up of mostly individual molecular chains (unimers) and very

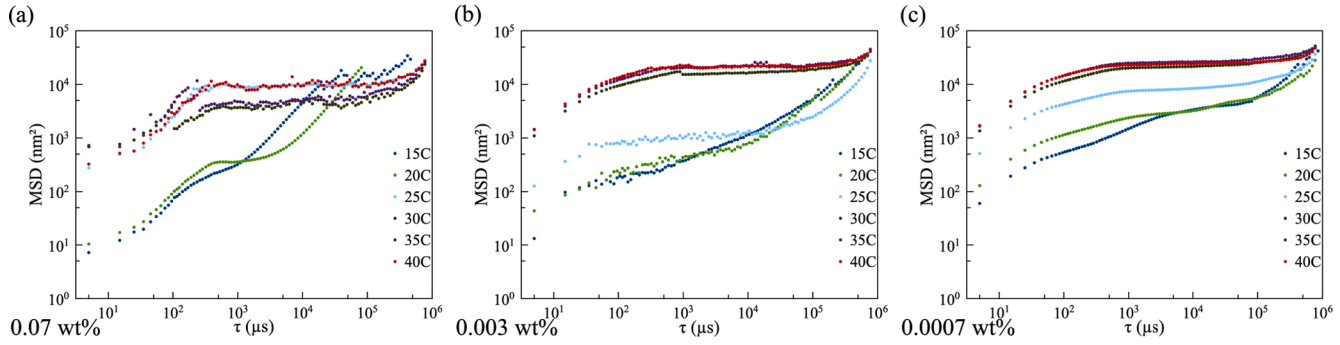

Fig. 7. Mean-squared displacement from DLS-microrheology on 20 wt% F127 solutions with probe particles of diameter of 2000 nm for probe particle concentrations of a) 0.07 wt%, b) 0.003 wt%, and c) 0.0007 wt%, at temperatures of 15–40 °C.

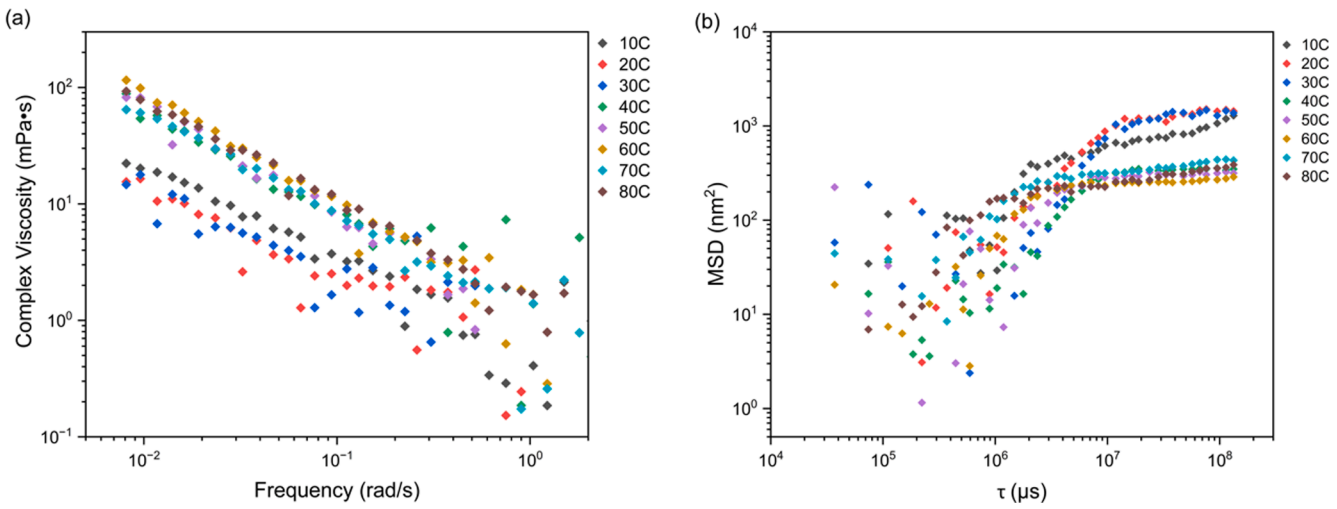

Fig. 8. The a) complex viscosity and b) mean squared displacement of 30 wt% F127 at temperatures between 10 °C and 80 °C from XPCS microrheology using 12 nm diameter SiO_2 particles.

few micelles, which seems to be restricting the Brownian motion of the small 12 nm probe particles. At 40 °C, we see by the rapid increase in the MSD over time that the probe particles are able to diffuse freely until around 8.3×10^6 μs where it starts to plateau at about 300 nm^2 just like in higher temperatures, which indicates that there is a mixture of free-flowing micelles and ordered structures, suggesting that gelation is still taking place at 40 °C.

4. Conclusion

In this work, we investigate a model thermoreversible polymeric hydrogel and compare results from DLS-microrheology with different size and concentrations of polystyrene probe particles and XPCS-microrheology with inorganic nanoparticles. Our results indicate that microrheological parameters derived from DLS and XPCS are influenced by size of probe particles. Somewhat surprisingly, we obtained trends that aligned most closely with the macroscopic rheology with probe particles of 40 nm, which are larger than the characteristic length scale of the gel structure of 11 nm but within the same order of magnitude. Utilizing larger probe particles, 2000 nm in size, yields microrheology data that are more dominated by elastic behavior than what we might expect from bulk rheology experiments. However, for these large particles, the particle concentration also impacts the measurement, particularly in when the F127 systems are in the sol state. We additionally performed XPCS-microrheology using probe particles that were similar in size to the F127 micellar length scale and found that the systems displayed more a more viscous response than would be expected based on the bulk rheology. These experiments demonstrate the utility of passive DLS- and XPCS-based microrheology in characterizing the rheological properties of complex polymeric biomaterials, while also highlighting important considerations in experimental design and choice of type, size, and concentration of probe particles used.

CRediT authorship contribution statement

Hengwei Zhu: Investigation, Formal analysis, Methodology, Writing – original draft. **Suan P. Quah-Ivarson:** Conceptualization, Methodology, Investigation, Formal analysis, Writing – original draft. **Yugang Zhang:** Methodology, Formal analysis, Software. **Andrei Fluerasu:** Methodology, Formal analysis, Software, Supervision. **Xiaoxi Yu:** Investigation. **Bingqian Zheng:** Investigation. **Xuechen Yin:** Investigation. **Weiping Liu:** Investigation. **Surita R. Bhatia:** Conceptualization, Funding acquisition, Project administration, Supervision, Writing – review & editing.

Declaration of Competing Interest

The authors declare that they have no known competing financial interests or personal relationships that could have appeared to influence the work reported in this paper.

Data availability

The raw/processed data required to reproduce these findings cannot be shared at this time as the data also forms part of an ongoing study.

Acknowledgments

We thank the organizers of this special issue in Honor of Dr. David Richens and the kind invitation to contribute. Financial support for this work was provided by National Science Foundation awards DMR-1905547, CBET-1903189, DGE-1922639, and CHE-1609494; NIH R01GM097971; ACS PRF award 55729-ND9; and a Department of Education Graduate Assistance in Areas of National Need (GAANN) fellowship for S.P.Q. and B.Z., Award P200A160163. This research used resources of the National Synchrotron Light Source II and Center for Functional Nanomaterials, U.S. Department of Energy (DOE) Office of Science User Facilities operated for the DOE Office of Science by Brookhaven National Laboratory under Contract No. DE-SC0012704.

Appendix A. Supplementary material

Supplementary data to this article, including additional microrheology results and comparison with bulk rheology data, can be found online at https://doi.org/10.1016/j.eurpolymj.2023.112434.

References

[1] P.R. Avallone, P. Iaccarino, N. Grizzuti, R. Pasquino, E. Di Maio, Rheology-driven design of pizza gas foaming, Phys. Fluids 34 (3) (2022).
[2] A.Z. Nelson, The Soft Matter Kitchen: Improving the accessibility of rheology education and outreach through food materials, Phys. Fluids 34 (3) (2022).
[3] C.E. Owens, M.R. Fan, A.J. Hart, G.H. McKinley, On Oreology, the fracture and flow of "milk's favorite cookie®", Phys. Fluids 34 (4) (2022).
[4] J.S. Saddik, R.H. Dave, Evaluation of powder rheology as a potential tool to predict tablet sticking, Powder Technol. 386 (2021) 298–306.
[5] Y.Z. Sinzato, F.R. Cunha, Capillary flow of magnetic fluids with effect of hydrodynamic dispersion, Phys. Fluids 33 (10) (2021).
[6] N. Sood, A. Bhardwaj, S. Mehta, A. Mehta, Stimuli-responsive hydrogels in drug delivery and tissue engineering, Drug Deliv. 23 (3) (2014) 748–770.

[7] J. Maldonado-Valderrama, J.M.R. Patino, Interfacial rheology of protein–surfactant mixtures, Curr. Opin. Colloid Interface Sci. 15 (4) (2010) 271–282.
[8] Z. Zhang, S. Barman, G.F. Christopher, The role of protein content on the steady and oscillatory shear rheology of model synovial fluids, Soft Matter 10 (32) (2014) 5965–5973.
[9] A. Wyma, L. Martin-Alarcon, T. Walsh, T.A. Schmidt, I.D. Gates, M.S. Kallos, Non-Newtonian rheology in suspension cell cultures significantly impacts bioreactor shear stress quantification, Biotechnol. Bioeng. 115 (8) (2018) 2101–2113.
[10] M.A. Raoufi, H.A.N. Joushani, S. Razavi Bazaz, L. Ding, M. Asadnia, M. Ebrahimi Warkiani, Effects of sample rheology on the equilibrium position of particles and cells within a spiral microfluidic channel, Microfluid. Nanofluid. 25 (9) (2021).
[11] B. Schroyen, D. Vlassopoulos, P. Van Puyvelde, J. Vermant, Bulk rheometry at high frequencies: a review of experimental approaches, Rheol. Acta 59 (1) (2019) 1–22.
[12] A. Dodero, R. Williams, S. Gagliardi, S. Vicini, M. Alloisio, M. Castellano, A micro-rheological and rheological study of biopolymers solutions: hyaluronic acid, Carbohydr. Polym. 203 (2019) 349–355.
[13] A. Habibi, C. Blanc, N.B. Mbarek, T. Soltani, Passive and active microrheology of a lyotropic chromonic nematic liquid crystal disodium cromoglycate, J. Mol. Liq. 288 (2019).
[14] W. Liu, B. Zheng, X. Yin, X. Yu, Y. Zhang, L. Wiegart, A. Fluerasu, B.L. Armstrong, G.M. Veith, S.R. Bhatia, XPCS microrheology and rheology of sterically stabilized nanoparticle dispersions in aprotic solvents, ACS Appl. Mater. Interfaces 13 (12) (2021) 14267–14274.
[15] R.M. Robertson-Anderson, Optical tweezers microrheology: from the basics to advanced techniques and applications, ACS Macro Lett. 7 (8) (2018) 968–975.
[16] Z. Xing, A. Caciagli, T. Cao, I. Stoev, M. Zupkauskas, T. O'Neill, T. Wenzel, R. Lamboll, D. Liu, E. Eiser, Microrheology of DNA hydrogels, PNAS 115 (32) (2018) 8137–8142.
[17] W. Liu, C. Wu, Rheological study of soft matters: a review of microrheology and microrheometers, Macromol. Chem. Phys. 219 (3) (2018).
[18] R.N. Zia, Active and passive microrheology: theory and simulation, Annu. Rev. Fluid Mech. 50 (1) (2018) 371–405.
[19] B.A. Krajina, C. Tropini, A. Zhu, P. DiGiacomo, J.L. Sonnenburg, S.C. Heilshorn, A. J. Spakowitz, Dynamic light scattering microrheology reveals multiscale viscoelasticity of polymer gels and precious biological materials, ACS Cent. Sci. 3 (12) (2017) 1294–1303.
[20] O.E. Cassidy, G. Rowley, I.W. Fletcher, S.F. Davies, D. Briggs, Surface modification and electrostatic charge of polystyrene particles, Int. J. Pharm. 182 (2) (1999) 199–211.
[21] P.C. Cai, B.A. Krajina, M.J. Kratochvil, L. Zou, A. Zhu, E.B. Burgener, P.L. Bollyky, C.E. Milla, M.J. Webber, A.J. Spakowitz, S.C. Heilshorn, Dynamic light scattering microrheology for soft and living materials, Soft Matter 17 (7) (2021) 1929–1939.
[22] S.P. Quah, Y. Zhang, A. Fluerasu, X. Yu, B. Zheng, X. Yin, W. Liu, S.R. Bhatia, Techniques to characterize dynamics in biomaterials microenvironments: XPCS and microrheology of alginate/PEO–PPO–PEO hydrogels, Soft Matter 17 (6) (2021) 1685–1691.
[23] B. Stoeber, C.-M.-J. Hu, D. Liepmann, S.J. Muller, Passive flow control in microdevices using thermally responsive polymer solutions, Phys. Fluids 18 (5) (2006).
[24] S. Liu, L. Li, Multiple phase transition and scaling law for poly(ethylene oxide)–poly(propylene oxide)–poly(ethylene oxide) triblock copolymer in aqueous solution, ACS Appl. Mater. Interfaces 7 (4) (2015) 2688–2697.
[25] K. Hyun, J.G. Nam, M. Wilhellm, K.H. Ahn, S.J. Lee, Large amplitude oscillatory shear behavior of PEO-PPO-PEO triblock copolymer solutions, Rheol. Acta 45 (3) (2005) 239–249.
[26] M. Jalaal, G. Cottrell, N. Balmforth, B. Stoeber, On the rheology of Pluronic F127 aqueous solutions, J. Rheol. 61 (1) (2017) 139–146.
[27] N. Gjerde, K. Zhu, B. Nyström, K.D. Knudsen, Effect of PCL end-groups on the self-assembly process of Pluronic in aqueous media, PCCP 20 (4) (2018) 2585–2596.
[28] J. Qu, X. Zhao, Y. Liang, T. Zhang, P.X. Ma, B. Guo, Antibacterial adhesive injectable hydrogels with rapid self-healing, extensibility and compressibility as wound dressing for joints skin wound healing, Biomaterials 183 (2018) 185–199.
[29] Z. Li, F. Zhou, Z. Li, S. Lin, L. Chen, L. Liu, Y. Chen, Hydrogel cross-linked with dynamic covalent bonding and micellization for promoting burn wound healing, ACS Appl. Mater. Interfaces 10 (30) (2018) 25194–25202.
[30] S. Chatterjee, P.C. Hui, C.W. Kan, W. Wang, Dual-responsive (pH/temperature) Pluronic F-127 hydrogel drug delivery system for textile-based transdermal therapy, Sci. Rep. 9 (1) (2019) 11658.
[31] T.G. Mason, Estimating the viscoelastic moduli of complex fluids using the generalized Stokes-Einstein equation, Rheol. Acta 39 (4) (2000) 371–378.
[32] T.G. Mason, D.A. Weitz, Optical measurements of frequency-dependent linear viscoelastic moduli of complex fluids, Phys. Rev. Lett. 74 (7) (1995) 1250–1253.
[33] E.M. Furst, T.M. Squires, Microrheology, Oxford University Press, 2017.
[34] M. Levin, G. Bel, Y. Roichman, Measurements and characterization of the dynamics of tracer particles in an actin network, J. Chem. Phys. 154 (14) (2021), 144901.
[35] Y.-L. Su, J. Wang, H.-Z. Liu, FTIR spectroscopic investigation of effects of temperature and concentration on PEO− PPO− PEO block copolymer properties in aqueous solutions, Macromolecules 35 (16) (2002) 6426–6431.